DAΦNE TECHNICAL NOTE

INFN - LNF, Accelerator Division

Frascati, March 14, 2001

Note: **L-33**

LINEAR OPTICS MODEL FOR DAΦNE MAIN RINGS

C. Biscari

Introduction

The linear optics model of the DAΦNE main rings has undergone several refinement procedures since the day-one commissioning.

Every magnetic element of the Main Rings has been measured, and the characteristic magnetic field calibrated against the power supply currents [1,2].

The first optical model was based on these calibrations. For the day-one commissioning phase the same model applied to both rings was accurate enough to tune the rings and optimise collisions. The rings had a two-fold symmetry, same optics for the two Interaction Regions. All the symmetries of the collider were maintained in the model, and the calibration constants were corrected by fitting betatron functions and dispersion measurements.

The installation of KLOE in spring 1999 changed the scenario. The rings lost the two-fold symmetry since the two IRs are different. The preliminary optical model, describing the rings with the model developed for the day-one configuration and completed with the nominal fields for solenoids and low-beta quads, showed to be accurate enough to describe both rings with tunes according with measurements at the level of ± 0.2 corresponding to ~4%.

Several configurations and working points have been applied and measured in the rings since the KLOE installation. From the analysis of these measurements the optical model has been refined more and more, passing through different phases: different models for the two rings, different calibration constants for each quadrupole, or types of quadrupoles, calibrations for KLOE and compensator solenoids.

From the optimisation procedures it can be concluded that a precise model of the rings must be different for the two rings. Furthermore the dependence on the orbit is not negligible.
Catia Milardi and Gabriele Benedetti have introduced the use of the LOCO code [3, 4], which fits the Response Matrix by adjusting the model parameters and their analysis confirms the above considerations.

It is clear that a tool describing both rings with the same formalism and parameters is very useful for the setting of the optics and the search for new working points. It is also clear that such a tool cannot be as precise as a model including the ring differences and the orbit dependence.

Using measurements done on both rings during last year I have developed a model fitting both rings for different configurations, except for the entrance/exit angles of the dipoles which differ by few mrad in the two rings description. The measurements done with the wigglers off and the wiggler fields lowered by 14% have been very useful since they have allowed me to separate the contribution of the wigglers to the arc optics from the contribution of the dipoles.

During the writing of this note several other configurations have been in the meanwhile applied to the rings and their analysis has allowed me to better refine the model. Measurements on non-linearities around the IR have also explained the behaviour of coupling, decoherence, tunes with the separation at the IP, and the difficulty to match betatron functions around the second IR with the same parameters for different vertical orbits.

In this note I will describe the present model characteristics, as it is at this stage. It is straightforward that the work will be continued, and updated with the future measurements of both rings.

Linear Model

The measurements used for modelling are:
* betatron functions, measured by the quadrupole gradient kick in each quadrupole
* dispersion function
* betatron tunes

The emittance obtained by the model is compared with the emittance measured at the Synchrotron Light Monitor (SLM) [5].

The momentum compaction α_c is compared with the one obtained from the measured synchrotron frequency:

$$\alpha_c \approx \left(\frac{f_{syn}}{f_{rev}}\right)^2 \frac{2\pi E_o}{heV} \approx 2.36\ 10^{-5} f^2_{syn}$$

at the usual V = 120 KV with f_{syn} in KHz.

The code MAD is used in the description of the rings.

A set of measurements corresponding to a single working point or a single configuration can be effectively fitted with MAD. Since the number of parameters is equal or larger than the measured data, it is always possible to obtain a good representation of the selected set of measurements.

The model then must be checked with a different set of measurements corresponding to other working points and configurations.

When different sets of measurements are used for the fitting, an iterative procedure must be used, in which the dependence of the fitted functions on each parameter must be taken into account, and opportunely weighted.

The present model has been developed on the positron ring using first the configurations without wigglers (three different working points), then three different sets with the wiggler on and finally one set with the wiggler field lowered by 14%. The results obtained have been checked with three configurations of the electron ring. The discrepancies observed have been used to change again the fitting parameters and so, in an iterative procedure, a solution has been found which is reasonable for all the cases taken into account.

In the usual configurations for KLOE data taking the two rings optics are different: they correspond to the better luminosity set-up, and differ not only in the tunes, but also in the arc optics. Set-ups with the same quadrupole configurations on both rings had been used and measured in the past, and differences between the two rings have always been observed since the day-one commissioning phase. They can be explained in part by the independently powered end poles of the wigglers, which were used to correct the orbits, or to different set-ups of the splitters. Since beginning of 2000 we have decided to keep all end-poles equals and the same for the splitters. Differences between the rings are still present, which can be explained by the stray fields from the transfer lines, the presence of Ion Clearing Electrodes, the sextupolar terms in some of the correctors.

The last measurements done on the rings without wigglers have shown that for the same quadrupole current configuration the two rings differs in their tunes by about 0.05 in the horizontal plane and five time less in the vertical one (positrons: 4.153, 4.206; electrons: 4.103, 4.194).

This means that the same model used for both rings will never describe them better than this 1% insofar as the betatron tune is concerned, unless the elements making the differences are included in the model.

The fit of the dispersion function is sensible to changes in the in/out angle between orbit and dipole faces to the order of few mrad. The fit of the dispersion functions in both rings has led to slightly different values of these parametes, which could effectively depend on the orbit.

I have chosen to treat the same kind of magnets with the same parameters, thus neglecting possible differences between elements corresponding to the same family, which could be important especially in wigglers, dipoles and compensators.

Errors and Precision in Measurements and Fits

The precision in the measurements of the betatron functions with the gradient kick method is essentially dominated by the thin lens approximation. Simulations show that the error in the betatron function value can reach values of ± 1 m, depending on the betatron function behaviour along the quadrupoles. The precision at minimum beta positions is poor and the values of the betatron function minima are more precise if extrapolated by the nearby peaks of the functions than if measured.

The errors coming from tune measurement are in comparison completely negligible, and those coming from uncorrected closed orbit are also negligible if the measurement is properly done, correcting the distortions within ± 0.2mm.

For a given quadrupole configuration the dispersion function depends on the corrector setting and on the coupling for an amount of the order of few cm (the maximum values of the dispersion in the ring are of the order of 2.5 m). Since the correctors are not included in the fit, the dispersion can be reproduced with a precision down of this order of magnitude.

The energy of the rings depends a little on the orbit and on the corrector settings (of the order of $\sim 2\ 10^{-3}$). The precise measurement of the energy is done only by KLOE energy scans around the Φ-resonance and is not available for all the configurations used.

The above considerations show that a single model will fit different structures at values not better than:

- ~ 0.05 betatron tunes;
- ~ 10% emittance and momentum compaction;
- ~ few cm in dispersion function;
- ~ 1m betatron functions at maximum positions, which means ~10% the values at low beta positions.

Description of the Model

The same linear model describes both rings with wigglers off / wigglers on / lowered field wigglers.

The model includes quadrupoles, solenoids, dipoles and wigglers. Correctors, skew quadrupoles and higher order multipoles are not included. The reference orbit corresponds to the nominal one.

Arc Quadrupoles

They are described by the rectangular model. Gradients and magnetic lengths correspond to the calibrations obtained with the magnetic measurement.

Quadrupoles are of two different types, small and large. The gradient dependence on the current is linear around the nominal values [2]: with the current I measured in A and the energy E in MeV:

$$K1\ (m^{-2}) = (9.1277*I + 4.53)/E \qquad \text{small}$$
$$K1\ (m^{-2}) = (16.963*I + 5.62)/E \qquad \text{large}$$

KLOE IR

Solenoids

Each solenoid (the KLOE one plus the two compensators) is represented by the product of solenoid matrices, 3 cm long, with longitudinal field which follows the measured solenoid field, corresponding to the magnetic measurement calibrations, assuming no saturation in the field. In all the configurations used the KLOE field corresponds to 2300 A, and the compensators to 77 A.

Permanent magnet quadrupoles

The low-beta quadrupoles of KLOE IR are inside the solenoid field of the detector. They are represented by thin lenses each 3 cm, interleaved to the solenoid matrices, whose strengths follow the measured gradient of each one of the three types of quadrupoles. Each lens is tilted by the tilted angle around which the quadrupoles have been aligned to better correct the coupling. An extra tilt, corresponding to the measured alignment [6] of the whole triplet, is added on both triplets. (parameters *deltas, deltal*). The gradient of each quadrupole is multiplied by a parameter used in the model fitting (*cc1, cc2, cc3*).

Coupling

The only source of coupling considered in this description is the one coming from the KLOE IR: solenoids and tilted quadrupoles. To reproduce the coupling as measured (values of the order of 0.3% have been observed), the tilts of the two IR triplets (*deltas, deltal*) have been used as parameters. Even if the measurement show that the two triplets are differently tilted [4], I have chosen a symmetric description around the IP to simplify the model and have *deltas = -deltal*. In this case I have neglected the measured coupling source coming from the second IR, since it has the same phase as the one coming from KLOE and is effectively corrected by the KLOE IR solenoid settings.

IR2

In the present IR2 there are two different types of quadrupoles: small and large aperture. The beams pass off axis. The IR transport matrix was first obtained by tracking the off-axis trajectories including fringing fields obtained fitting the measured gradient [7]. Each quadrupole was then represented by a rectangular model quadrupole matrix with the gradients, which better fitted the so obtained transport matrix. On these gradients a calibration parameter (*Perir*2, 3, 4) has been used for the model.

Dipoles

The bending dipoles are of four different types, plus the splitter magnets around the Interaction Regions. Their design parameters are (the parameters have the same meaning of the MAD input deck):

Table I - Nominal parameters of dipoles

TYPE	L_{mag} (m)	Angle (°)	ρ(m)	$\varepsilon_1,\varepsilon_2$ (°)	FINT
Short sector	0.99	40.5	1.4006	0.,0	0.040
Short rectangular	0.99	40.5	1.4006	20.25, 20.25	0.043
Long sector	1.21	49.5	1.4006	0,0	0.041
Long rectangular	1.21	49.5	1.4006	24.75, 24.75	0.047
Splitters	1.45	8.749	9.4955	0, 8.749	

The magnetic length and the radius of curvature in the model are the nominal ones. The transport matrices are fitted by adding a thin lens at each dipole end, corresponding to an increment in the angles $\Delta\varepsilon_1$, $\Delta\varepsilon_2$, and by changing the fint values. The splitters maintain the nominal values.

Wigglers

Each one of the four wiggler per ring consists of five central poles (L ~32cm), and two half poles (L~16cm) on each side. The central poles of the four wigglers of one ring are powered as a family; each pair of end poles are individually powered.

Each pole is represented by three dipoles [8], the lateral ones having half the field of the central one and half the magnetic length, to take into account the rapid decrease of the field in between two poles.

The end poles are also represented by three dipoles, with the magnetic length of the central part equal to the lateral ones.

Each dipole is represented by a sector magnet with two thin lenses at the end to adjust both vertical and horizontal focusing. The fint lens is placed only on the central dipole of each pole, and scaled with the corresponding bending angle.

The sextupole term of the wiggler field [9] acts like a defocusing quadrupole on the off-axis trajectory and is added in the thin lenses at each dipole end. It increases by ~ 25% the value corresponding to the rectangular magnet for the nominal magnetic field. For wigglers working with lower fields, this term scales differently for positive and negative poles, since it depends on the trajectory inside the pole. The nominal trajectory is centred on the wiggler axis only at the maximum field value. Lowering the field, the trajectory excursion on the positive poles is smaller than in the negative ones, where it remains constant. This fact is taken into account in the model by correcting with the field the strength of the extra quadrupole term differently in positive and negative poles.

The free wiggler parameters in the model are three: a parameter multiplying the central pole end faces (*deps*), one for the end poles end faces (*pt*) and the fint of the whole wiggler (*fw*). The following Table II is the wiggler description as written in the MAD input format. The parameter '*campo*' is unity for the nominal magnetic field. The field at which the wigglers are normally powered corresponds to a sligtly lower value by 0.2% (*campo = 0.998*).

Table II – Wiggler description in MAD formalism

```
campo=1.

FINTW = fw/(2*0.01)
fcurv=campo*510/e

teta=0.0850*fcurv

eps1p= (0.0213*deps*fcurv) + (0.0053)*depqp*fcurv
eps2p= (0.0850*deps*fcurv) + (0.0210)*depqp*fcurv
eps1m= (0.0213*deps*fcurv) + (0.0053)*depqm*fcurv
eps2m= (0.0850*deps*fcurv) + (0.0210)*depqm*fcurv

tetat=teta
eps1t=eps1m*pt

lW1f=0.08024392
lW2f=LW1F/2

lgr=0.080267

! end poles
Wf1:SBEND,L=lw1f,ANGLE=-tetat/2,E1=-eps1t ,E2=-eps1t
Wf2:SBEND,L=lw2f,ANGLE=-tetat/2,E1=-eps1t,E2=eps1t,fint=1.*fintw/2,hgap=0.01
Wf3:SBEND,L=lw1f,ANGLE=-tetat/2,E1=-eps1t ,E2=-eps1t

! positive poles
Wp1: SBEND,L=lgr,ANGLE=teta/2.,E1=eps1p ,E2=eps1p
Wp2: SBEND,L=2*lgr,ANGLE=2*teta,E1=eps2p ,E2=eps2p,fint=1.*fintw,hgap=0.01
Wp2a: SBEND,L=lgr,ANGLE=teta  ,E1=eps2p, fint=1.*fintw/2,hgap=0.01
Wp2b: SBEND,L=lgr,ANGLE=teta  ,E2=eps2p, fint=1.*fintw/2,hgap=0.01

! negative poles
Wm1: SBEND,L=lgr,ANGLE=-teta/2.,E1=-eps1m ,E2=-eps1m
Wm2: SBEND,L=2*lgr,ANGLE=-2*teta,E1=-eps2m  ,E2=-eps2m,fint=1.*fintw,hgap=0.01

WIGfr1: LINE=(Wf1,Wf2,Wf3)
WIGfr2: line=(Wf3,Wf2,Wf1)

WIGp: LINE=(Wp1,Wp2,Wp1)
WIGm: LINE=(Wm1,Wm2,Wm1)

WA: LINE=(WIGfr1,WIGp,WIGm,Wp1,Wp2a)
WB: LINE=(Wp2b,Wp1,WIGm,WIGp,WIGfr2)

Wiggler: LINE=(WA,WB)
```

Configurations of the Rings

Nine different configurations of the positron ring and three of the electron one have been considered. In Table III the date, the dataset and the file containing the betatron function measurements are listed.

Table III - Configurations of the positron ring

	configuration	date	dataset	beta measurements
e+				
a	KLOE – w.p.	30-10-00	pMRp_2000103003pom30	positroni30mat
b	KLOE – w.p.	23-11-00	pMRp_2000112309unoEottantaquattro	
c	'Ideal d.a.'	23-11-00	pMRp_2000112313id7	ideale
d	Half integer	09-11-00	pMRp_2000110922misure_beta	12_64psera9
e	wgls 86%	15-12-00	pMRp_2000121509wigg82dc	wig82dc_p
f	wgls 86%	26-02-01	pMRp_2001022601buttami	buttami
g	wgl off 4.64 3.95	28-11-00	pMRp_2000112815crom1	wig0crom1
h	wgls off 4.64 4.21	30-11-00	pMRp_2000113008woff30n	
i	wgls off 4.15 4.21	01-12-00	pMRp_2000120112NW1521corr	WN 15_21
e-				
A	KLOE – w.p.	19-10-00	eMRe_2000101902mattina19	giovPom_e
B	low emittance	06-10-00	eMRe_2000100601misbeta_lowemitt	lowemitt08
C	wgl off 4.12 4.19	19-02-01	eMRe_2001021914misure_beta	betawigoffE

Model Parameters

The following Table IV summarises the model parameters. The first column shows the default values, corresponding to the calibrations from the magnetic measurements, or to the alignment measurements. In the second column the values of the present model are listed. In the fourth column the magnet to which the parameter refers is listed.

The values of $\Delta\varepsilon_i$ for the electrons refer only to the structures with wigglers on (A and B), the structure with wigglers off C) has the same parameters of the positron ring.

Table IV - Model parameters

Parameter	Nominal	Model	
cc1	1	1.015	KLOE IR quadK3, K4
cc2	1	1.000	KLOE IR quadK2, K5
cc3	1	1.030	KLOE IR quadK1, K6
deltal	-0.7°±0.1	-1.17°	tilt of quads K1,K2,K3
deltas	1.0°±0.1	1.17°	tilt of quads K4,K5,K6
perir2	1	0.985	IR2 quad i2003,2005
perir3	1	0.982	IR2 quad i2002,2006
perir4	1	0.985	IR2 quad i2001,2007
$\Delta\varepsilon_1$ e+ (rad) e-	0.0	0.022 0.027	Short sector dipole
$\Delta\varepsilon_2$ e+ (rad) e-	0.0	-0.020 -0.015	Short rect dipole
$\Delta\varepsilon_3$ e+ (rad) e-	0.0	0.020 0.022	Long sector dipole
$\Delta\varepsilon_4$ e + e-	0.0	-0.038 -0.043	Long rect dipole
$Fint_1$	0.040	0.052	Short sector dipole
$Fint_2$	0.043	0.052	Short rect dipole
$Fint_3$	0.041	0.065	Long sector dipole
$Fint_4$	0.047	0.039	Long rect dipole
deps	1.0	1.000	wiggler central poles
pt	1.0	1.140	wiggler end poles
fw	0.0	-0.007	wiggler fint

Results

Table V summarises the results for the twelve configurations taken into account. The measured values together with the values calculated with the model are shown. For some configurations the best fit corresponds to a modified energy (*deltap* = $\Delta p/p$). In the Appendix the figures show the measured betatron functions and dispersion (*) together with the calculated functions using the model.

The first structure with wigglers lowered at 86% ("e") does not match with the model. It could be due to a not well corrected orbit. In the Appendix there are two different figures corresponding to configuration "e". One refers to the same model used for all configurations; the other one is obtained by changing the wiggler parameters. The configuration "f", whose orbit has been better corrected, fits well the model.

Table V - Summary of results

	lattice	**a**	**b**	**c**	**d**	**e**	**f**	**g**	**h**	**i**	**A**	**B**	**C**
		e+	e+	e+	e+	e+	e+	e+	e+	e+	e-	e-	e-
		KLOE	KLOE	ideal	half	wiggler	wiggler	wig off	wig off	wig off	KLOE	low	wgl off
M	date	**30-10-00**	**23-11-00**	**23-11-00**	**09-11-00**	**15-12-00**	**26-02-01**	**28-11-00**	**30-11-00**	**01-12-00**	**19-10-00**	**06-10-00**	**19-02-01**
E	Q_x	5.155	5.152	5.154	4.647	5.150	5.08	4.636	4.641	4.153	5.115	5.115	4.12
A	Q_y	5.214	5.212	5.213	5.121	5.195	5.13	3.948	4.219	4.206	5.194	5.194	4.19
S	f_s	31.0	31.0	35.0	29.5	27.7		33.3	27.7	37.2	33.0	30.6	37.5
U	α_c	.0227	.0227	.0289	.0205	.0181		.0262	.0181	.0327	.0257	.0221	.035
R	ε_x		.86	.90									
E	f_{rf} (kHz)	.259	.259	.259	.259	.263	.263	.410	.410	.410	.259	.259	.410
M	deltap	0.001	0.000	0.000	0.000	-0.002	0.0035	0.0035	0.001	0.000	0.000	0.000	-0.002
O	Q_x	5.158	5.155	5.141	4.621	5.093	5.101	4.638	4.654	4.149	5.125	5.120	4.176
D	Q_y	5.211	5.202	5.217	5.122	5.202	5.160	3.949	4.226	4.201	5.204	5.195	4.198
E	α_c	.0295	.0288	.0300	.0251	.0282	.036	.0263	.0187	.0324	.0329	.0251	.0320
L	β^*_x (m) I1	5.2	5.1	4.2	5.0	4.8	9.4	3.7	4.4	3.7	4.1	5.1	4.1
L	β^*_y (cm) I1	7.8	7.2	6.5	6.0	7.4	4.5	11.2	7.1	6.6	6.5	5.7	8.3
I	β^*_x (m) I2	4.6	4.6	3.7	4.4	3.4	7.8	3.5	3.8	3.3	4.2	4.4	3.8
N	β^*_y (cm) I2	8.5	10.2	9.9	8.4	7.9	6.9	15.0	9.1	9.7	8.0	8.4	9.8
G	ε_x(mm mrad)	1.02	.99	.80	.82	.86	.49	.59	.57	.79	1.11	.60	.73
	τ_x(msec)	42	42	41	41	49	49	106	95	100	41	41	99
	τ_y(msec)	36	36	36	36	42	42	75	76	77	36	36	77
	τ_z(msec)	17	17	17	17	20	20	33	39	34	17	17	34

In Fig. 1 the differences (both absolute and relative) between the measured tunes and the modelled ones are plotted.

Figure 2 shows the difference between the momentum compaction measured and modelled.

Figures 3 and 4 show the betatron functions at both IPs as calculated from the model.

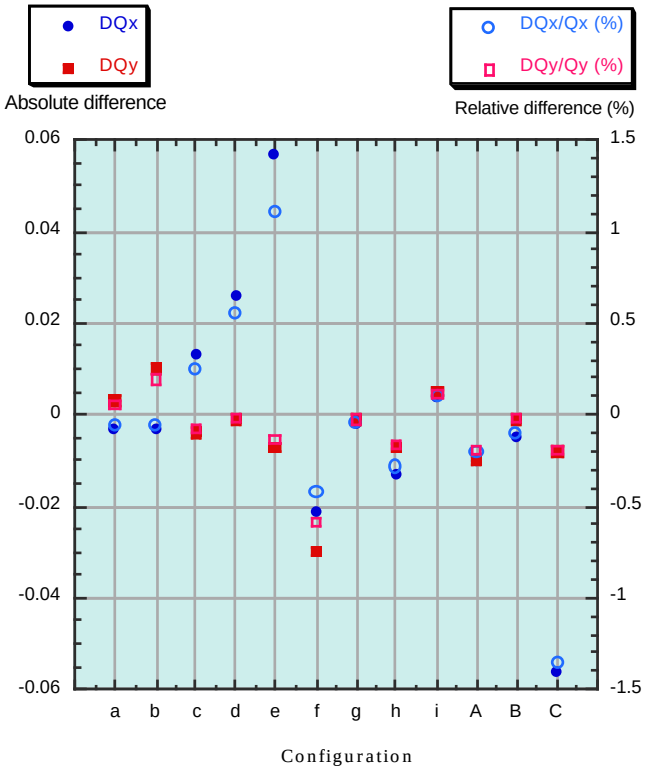

Figure 1 – Absolute and relative difference beween measured/modelled betatron tunes for the 12 configurations.

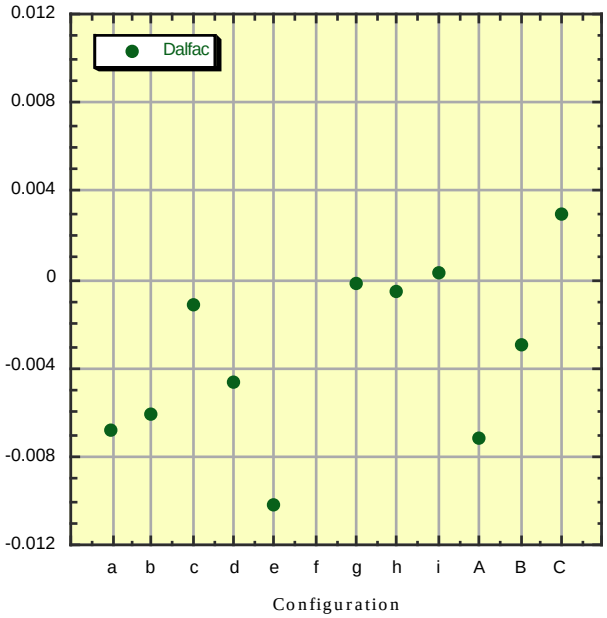

Figure 2 - Absolute difference beween measured/modelled momentum compaction for the 12 configurations.

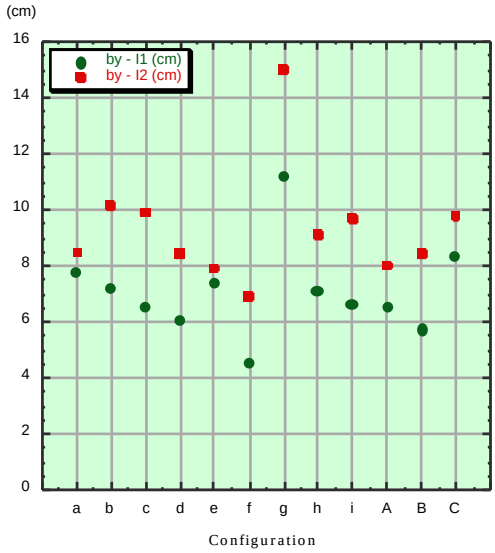

Figure 3 – β_y* in both IPs (model

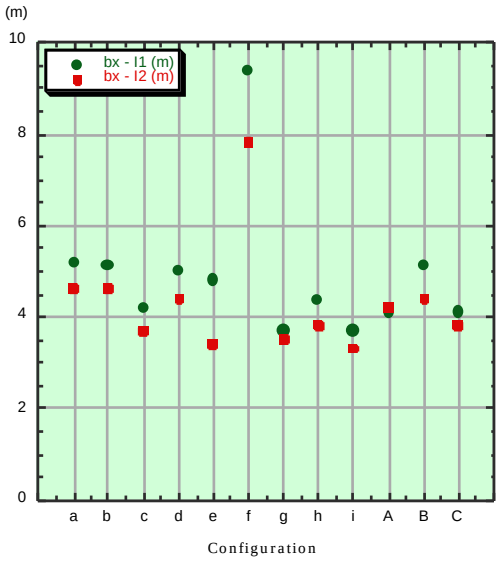

Figure 4 – β_x* in both IPs (model)

References

[1] C. Biscari, M.A. Preger: "Numerical constants and initial set points for the first part of the DAΦNE injector commissioning", DAΦNE Technical Note C-17 (1996).

[2] S. Guiducci, M.A. Preger: "Calibration constants and nominal set points for the day-one latttice of the DAΦNE main rings", DAΦNE Technical Note C-18 (1997).

[3] J. Safranek: "Experimental determination of storage ring optics using orbit response measurements" Nuclear Instruments & Methods in Physics Research A 338 (1997) 27-36.

[4] G. Benedetti: "Modello dell'ottica lineare di DAΦNE ", Tesi di Laurea, Università di Firenze, in preparation.

[5] A. Ghigo, F. Sannibale, M. Serio: "Synchrotron Radiation Monitor for DAΦNE", AIP Conference Proceedings 333 - Beam Insrumentation Workshop, Vancouver, B.C., Canada October 1994, p. 238.

[6] F.Sgamma, M. Paris, M. Troiani: Zona di Interazione di KLOE: "Misure di Febbraio e Riallineamento di Marzo 2000", DAΦNE Technical Note ME-9 (2000).

[7] C.Biscari - "Low Beta Quadrupole Fringing Field on Off-Axis Trajectory" - Proceedings of the Workshop on Non Linear Dynamics in Particle Accelerators (to be published) - Arcidosso (Italy), sept. 1994 (DAΦNE TECHNICAL NOTE L-20 (19.12.1994))

[8] B. Bolli, N. Ganlin, F. Iungo, F. Losciale, M. Paris, M. Preger, C. Sanelli, F. Sardone, F. Sgamma, M. Troiani: " The Dipoles of The DAΦNE Main Ring Achromats", DAΦNE Technical Note MM-26 (1997).

[9] M. Bassetti, C. Biscari, M.A. Preger: "Optical Characteristics of the DAΦNE Wiggler", DAΦNE Technical Note G-27 (1994).

APPENDIX

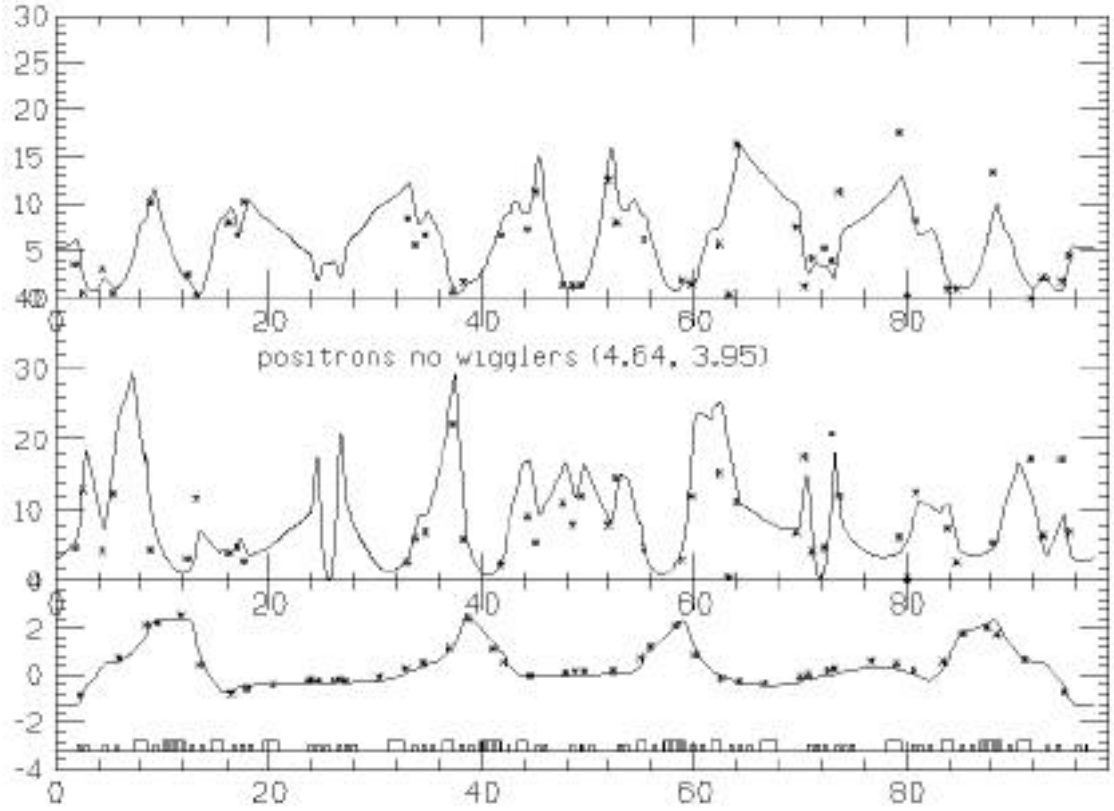

Configuration "**d**"

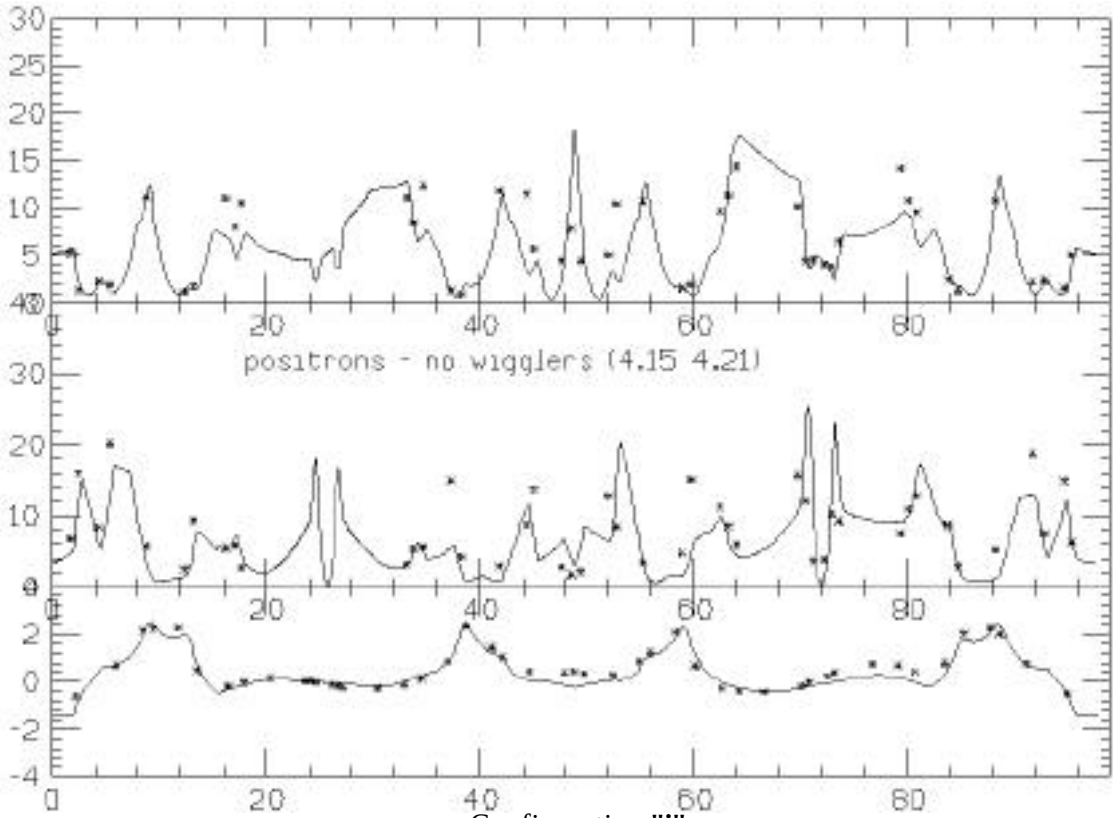

Configuration "**i**"

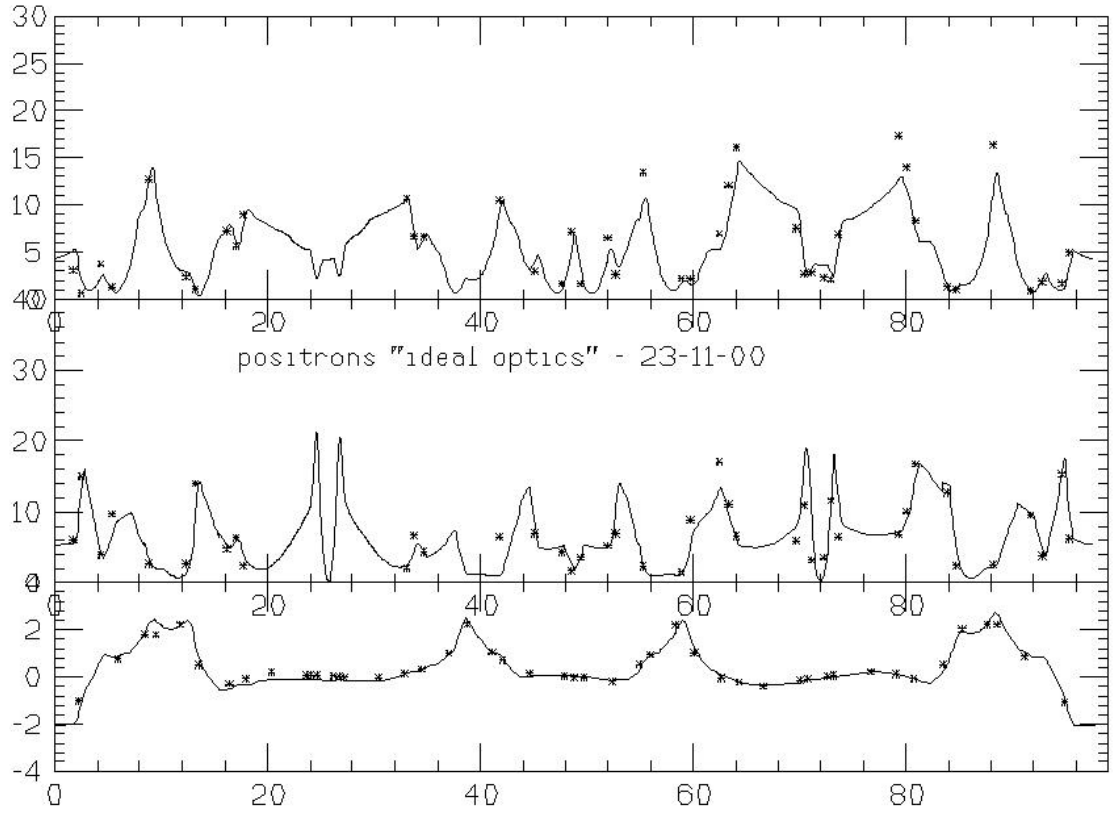

Configuration "**c**"

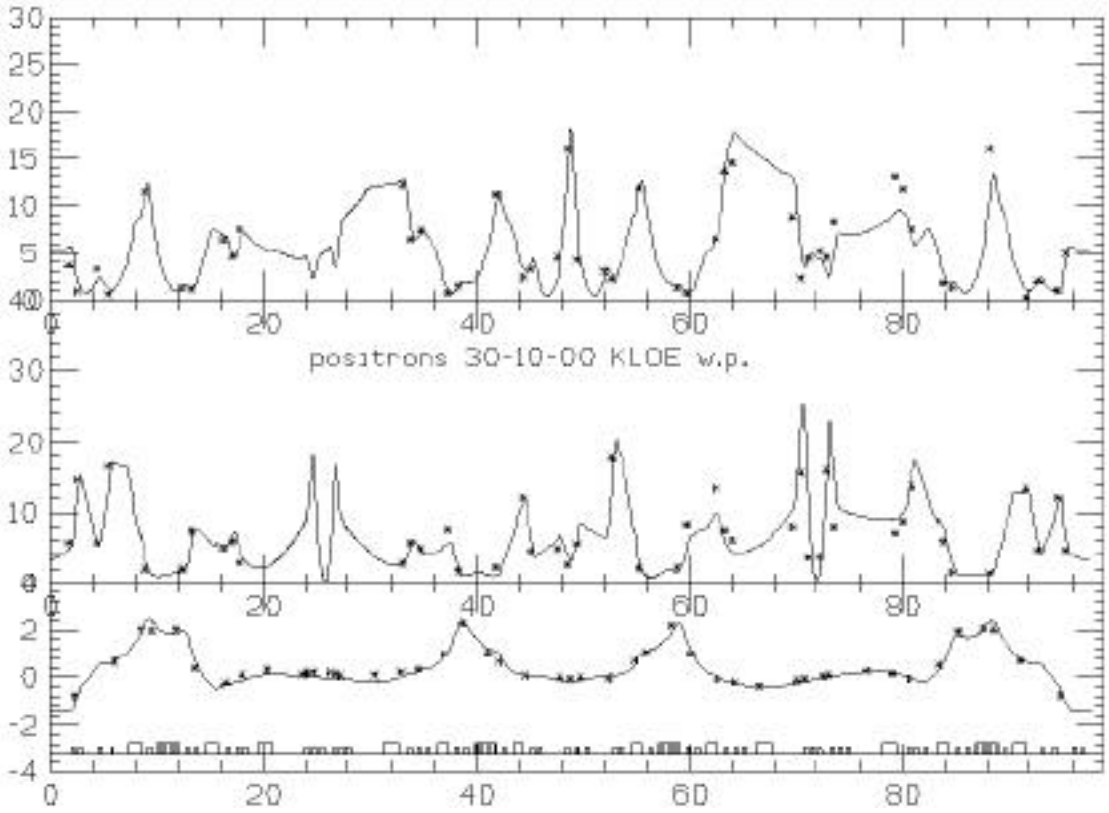

Configuration "**a**"

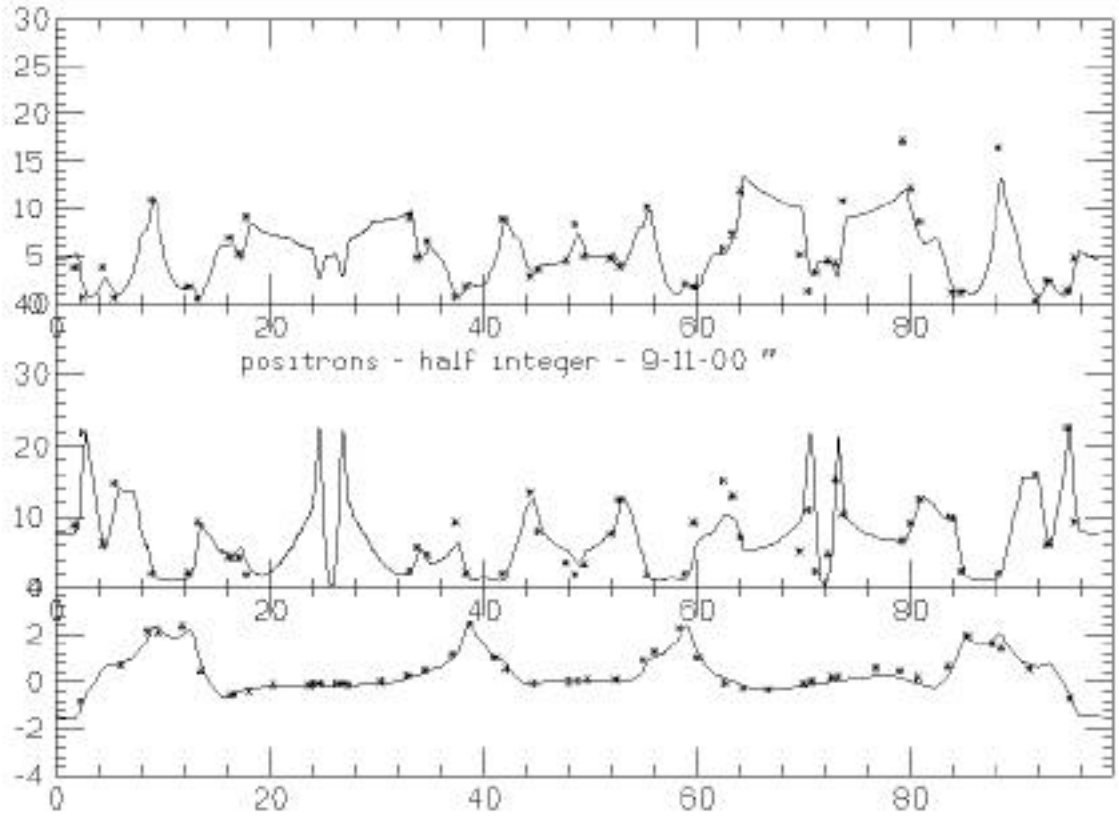

Configuration "**d**"

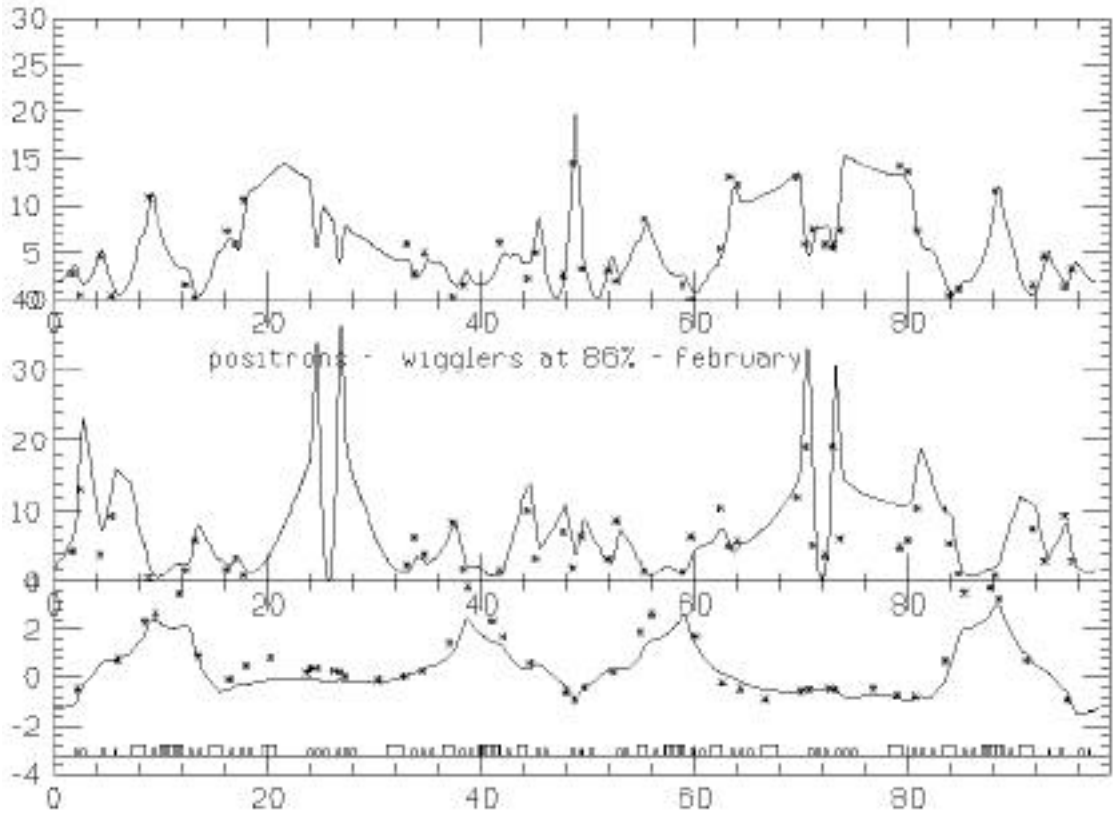

Configuration "**f**"

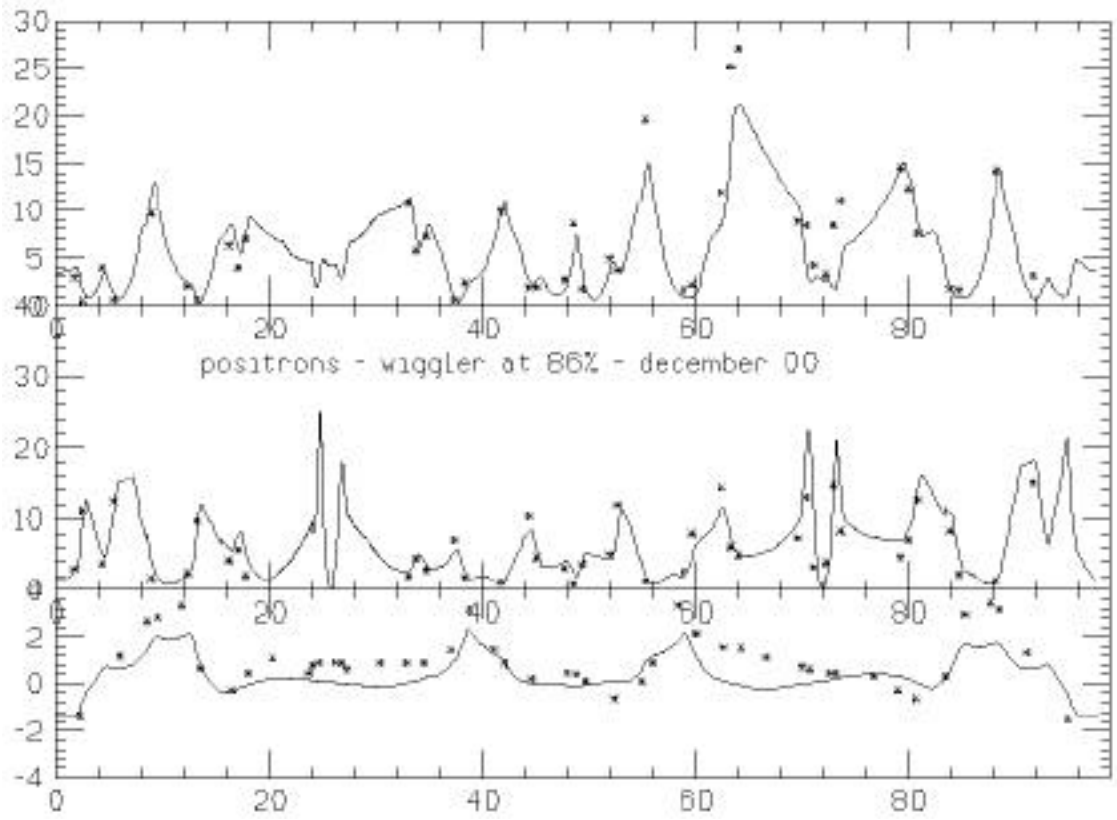

Configuration "**e**" - different model

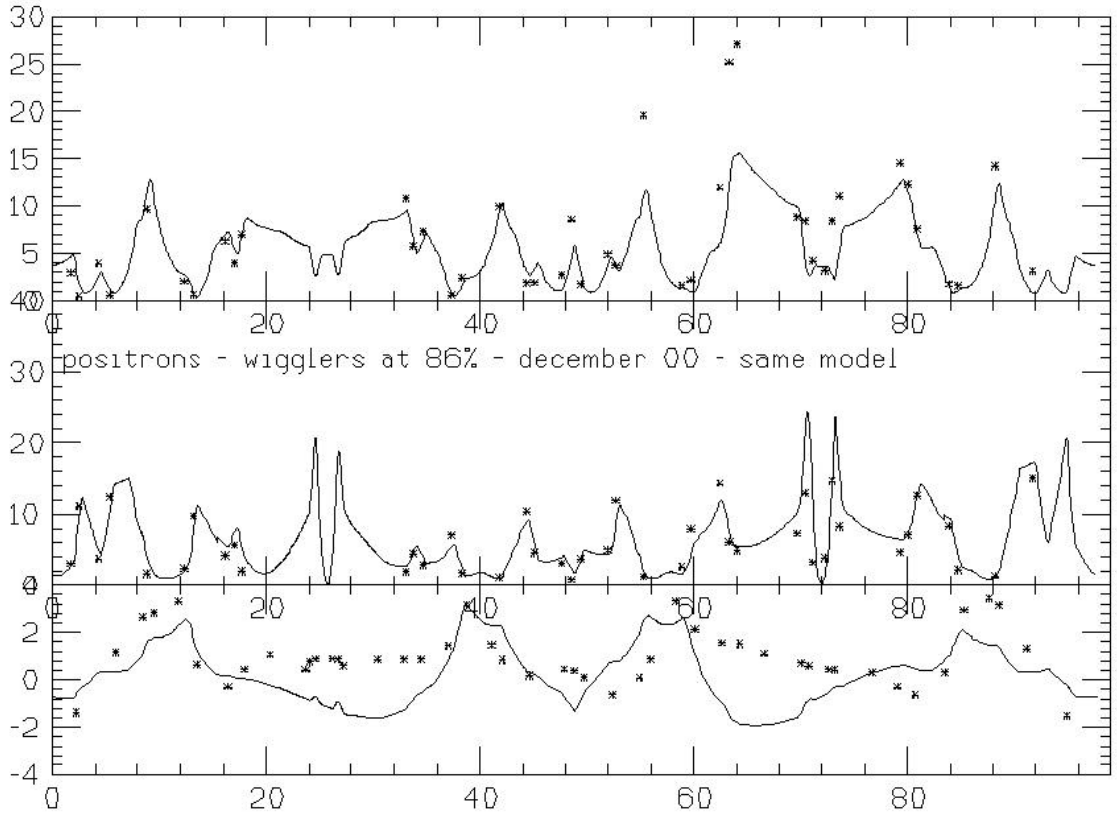

Configuration "**e**"

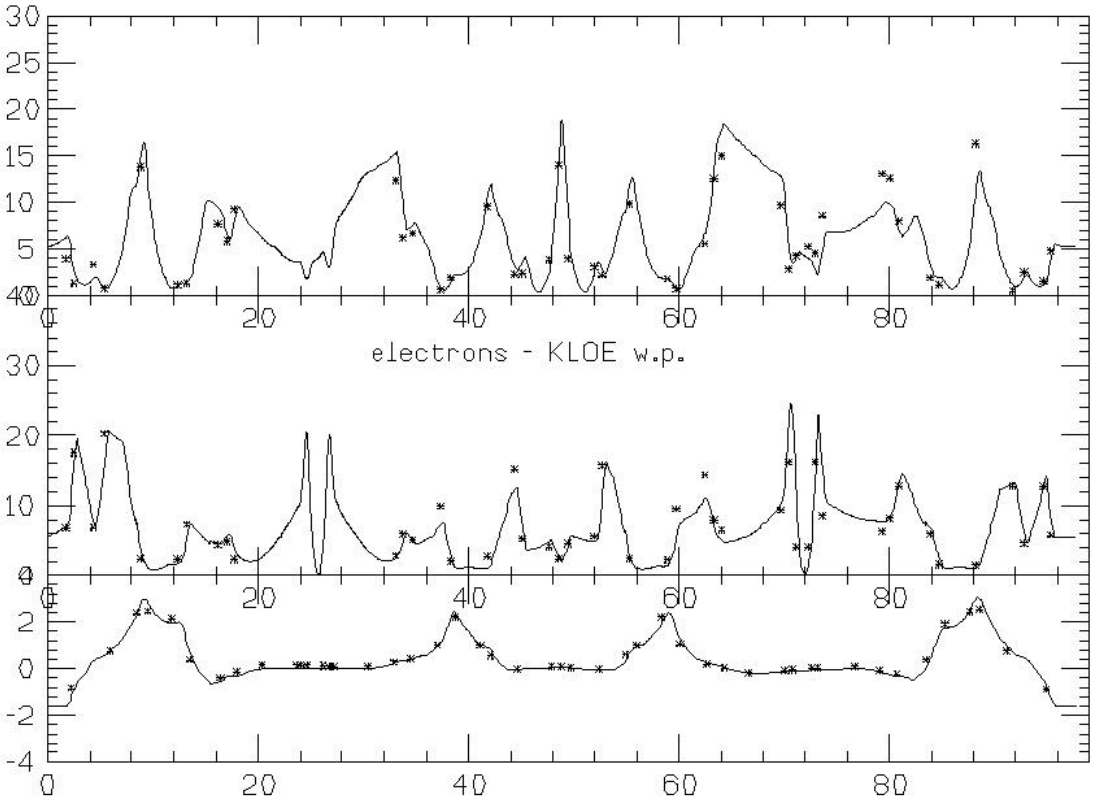

Configuration "**A**"

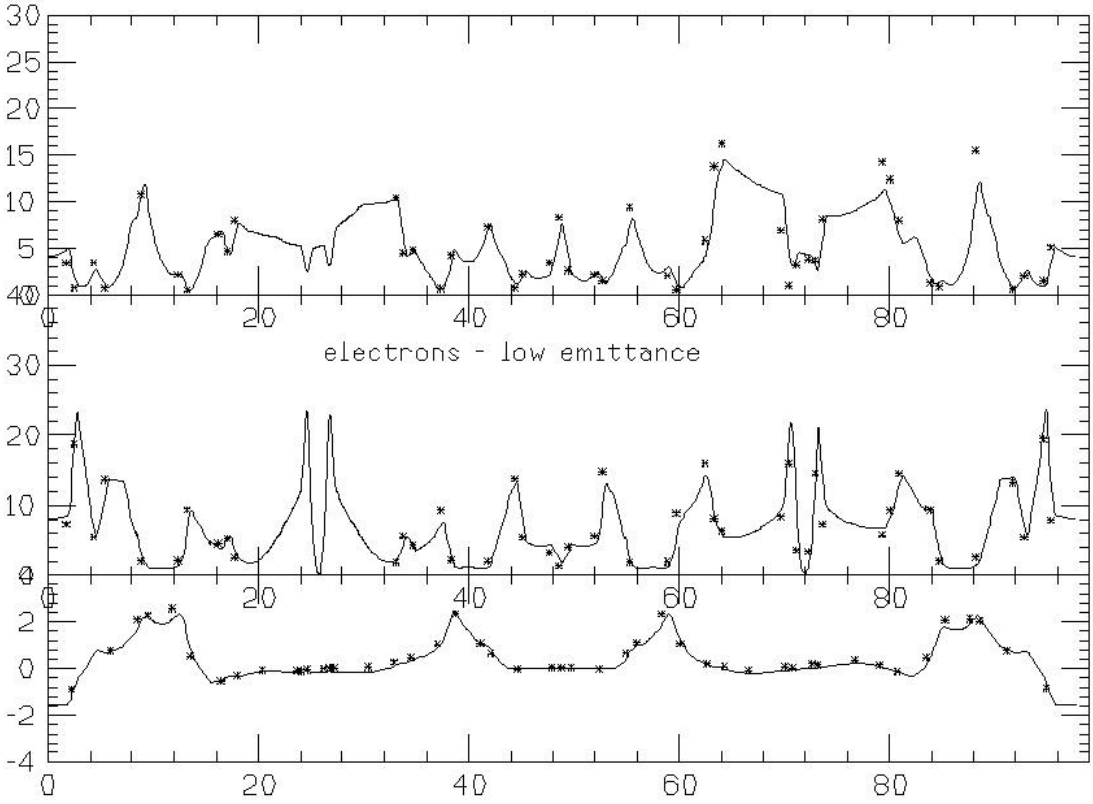

Configuration "**B**"

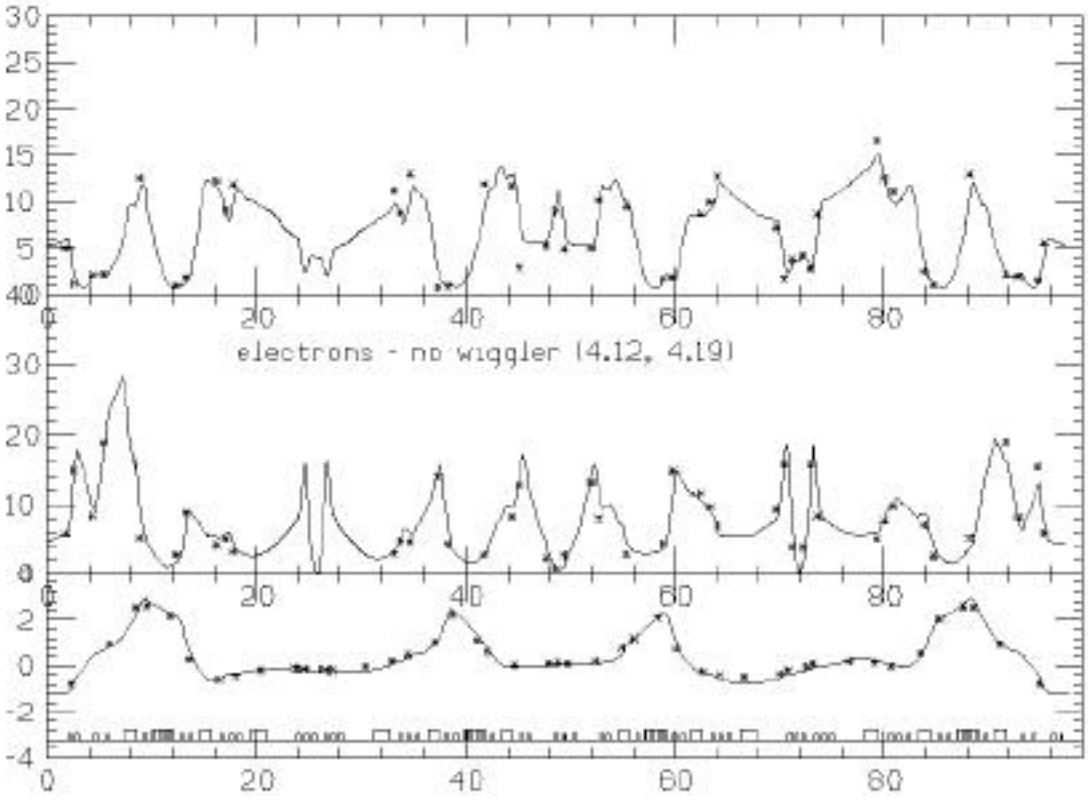

Configuration "**C**"